

# A Physical Interpretation of Recent Tropical Cyclone Post Landfall Decay

L. M. Phillipson<sup>1</sup> and R. Toumi<sup>1</sup>

<sup>1</sup>Space and Atmospheric Physics Group, Department of Physics, Imperial College London, London, UK.

## Key Points:

- A simple physically based vortex decay model of maximum surface winds was utilised to investigate post-landfall decay.
- The decay parameter obtained from the model has been decreasing from 1980 to 2018.
- A global mean increase of wind speed 24 hours after landfall is consistent with this slower decay.

---

Corresponding author: Luke Phillipson, [l.phillipson14@imperial.ac.uk](mailto:l.phillipson14@imperial.ac.uk)

## 12 Abstract

13 The decay of landfalling tropical cyclones (TCs) is important to the damage caused.  
 14 We examine a simple physically based decay model of maximum surface winds driven  
 15 by frictional turbulent drag and a modification accounting for partial to complete land  
 16 roughness. The model fits an algebraic decay with a parameter determined by the ra-  
 17 tio of the surface drag coefficient to the effective vortex depth. This parameter has been  
 18 decreasing from 1980 to 2018. There is also a global mean increase of wind speed 24 hours  
 19 after landfall of +1.13 m/s per decade. We cannot exclude the possibility that this trend  
 20 is driven by the initial wind speed increase, but it is most likely due to a slowing of the  
 21 decay. This weaker decay amounts to an additional 7 hours of gale force winds for a typ-  
 22 ical Category 1 at landfall.

## 23 1 Introduction

24 The inland effects of major tropical cyclones (TC) can be devastating (Coch, 2020).  
 25 An increase of inland risk is implied by recent trends of intensification over the ocean  
 26 (Bhatia et al., 2019; Wang et al., 2020), coastal migration (Wang & Toumi, 2021) and  
 27 slowing land decay (Li & Chakraborty, 2020). A combination of factors are thought to  
 28 control the decay of TCs after landfall including the reduction of surface moisture fluxes  
 29 and increased frictional dissipation from the rougher land (Chen & Chavas, 2020). A sim-  
 30 ple empirical exponential model of post landfall decay (Kaplan & DeMaria, 1995) has  
 31 been widely used operationally within the Statistical Hurricane Intensity Prediction Scheme  
 32 (SHIPS) (DeMaria et al., 2005), typhoon prediction scheme of Knaff et al. (2005) and  
 33 the Southern Hemisphere Statistical Typhoon Intensity Prediction Scheme (SH STIPS)  
 34 (Knaff & Sampson, 2009). In stochastic risk modelling the exponential model is also used  
 35 Bloemendaal et al. (2020). In regional studies the exponential model has been applied  
 36 to case studies for New England, USA (Kaplan & DeMaria, 2001), India (Bhowmik et  
 37 al., 2005) and Southern China (Wong et al., 2008) landfalls. In a recent trend analysis,  
 38 the exponential model was used to infer a recent slowing of land decay of hurricanes (Li  
 39 & Chakraborty, 2020). Several refinements have been considered by including an adjust-  
 40 ment to the initial landfall wind speed, consideration of islands (DeMaria et al., 2006)  
 41 and a pressure filling variant (Vickery, 2005).

42 Despite the extensive use of the exponential model, an empirical model can only  
 43 provide limited understanding of the decay problem. Furthermore, theoretical studies  
 44 of the spin-down of geophysical vortices by Greenspan and Howard (1963) and Eliassen  
 45 (1971) have demonstrated that the exponential decay of the tangential winds is strictly  
 46 only valid for a laminar boundary layer. Therefore the assumption of a simple exponen-  
 47 tial decay is questionable for TC environments with shear-driven turbulent flow (Montgomery  
 48 et al., 2001). An alternative for a turbulent flow regime would be in the form first the-  
 49 orized by Eliassen (1971) and expanded in Eliassen and Lystad (1977), predicting an al-  
 50 gebraic temporal decay. This theory was later validated by Montgomery et al. (2001)  
 51 for modelled hurricane strength vortices over the ocean. Smith and Montgomery (2008)  
 52 and Vogl and Smith (2009) cast doubt over some of the linearity assumptions. Never-  
 53 theless the simplicity of the analytic model is attractive to provide a physical interpre-  
 54 tation of the observed TC decay over land. Here, we examine, for the first time, this de-  
 55 cay model against global landfall data, propose a modification and finally find recent changes  
 56 in observed post landfall wind speeds.

## 57 2 Methods

### 58 2.1 Decay Models

59 The algebraic decay model (ALG) is based on quadratic form of the turbulent drag;

60 
$$\frac{dv}{dt} = -Kv^2 \quad (1)$$

61 with the solution;

62 
$$\frac{1}{v_t} = \frac{1}{v_0} + Kt \quad (2)$$

63 where  $v_t$  is the maximum tangential surface wind speed at some time  $t$ ,  $v_0$  is the  
64 initial tangential surface wind speed at landfall ( $t = 0$ ) and  $K$  is the decay parameter  
65 defined as;

66 
$$K = \frac{C_D\chi}{H} \quad (3)$$

67 where  $C_D$  is the surface drag coefficient,  $\chi$  is the ratio of tangential winds at the  
68 surface to the top of the boundary layer.  $H$  is the effective height of the vortex and refers  
69 to the depth of over which the friction acts to spin down the vortex. The half life can  
70 also be found from Eq. 2;

71 
$$t_{1/2} = \frac{1}{v_0K} \quad (4)$$

72 where  $t_{1/2}$  is the time to half intensity from initial maximum wind intensity ( $v_0$ ).  
73 The decay parameter,  $K$ , determines the rate of the decay. A rougher surface (large  $C_D$ )  
74 increases the rate of the decay while a larger depth,  $H$ , decreases the rate of decay. This  
75 is physically sensible as a rougher surface causes more friction and a larger effective vor-  
76 tex height would take longer to spin-down.

77  $K$  may increase during the transition from ocean to land because  $C_D$  can be ex-  
78 pected to increase. During the early stages of landfall,  $C_D$  transitions from lower val-  
79 ues over the smoother ocean to higher values over rougher land. This transition is how-  
80 ever not instantaneous with some proportion of the cyclone remaining over the ocean  
81 at landfall. The exact values of  $C_D$ ,  $\chi$  and  $H$  for transitioning to over land are unknown  
82 for each individual case. In this framework  $H$  stays the same as the wind speed decays,  
83 representing an average  $H$  during the decay within the model fitting. In reality  $H$  may  
84 also decrease. It is also difficult to quantify any change in  $\chi$  for the transition.

85 DeMaria et al. (2006) suggested that the decay is slower if a portion of the storm  
86 remained over the ocean and accounted for this transition by modifying the exponen-  
87 tial model of (Kaplan & DeMaria, 1995). Here we account for changes in turbulent drag  
88 over the ocean and land. Therefore, assuming the same symmetry at landfall ( $t = 0$ )  
89 half of the the cyclone is over the ocean. We then assume that the initial decay param-  
90 eter  $K$  is only half ( $K/2$ ) of it's final value  $K$  at some time  $t_s$  when the entire cyclone  
91 is fully over the land. We do not set  $t_s$  as a function of radius and translation speed and  
92 instead allow  $t_s$  to become an extra parameter to be fitted. This means we do not need  
93 the radius which is rarely observed.  $K$  is set to relax exponentially from  $K/2$  to  $K$  over  
94 this transitional timescale  $t_s$ . For the case of a landfalling TC the modified decay model  
95 (ALG-t) becomes;

96 
$$\frac{dv}{dt} = -K\left(1 - \frac{1}{2}e^{-t/t_s}\right)v^2 \quad (5)$$

97 with a solution;

$$\frac{1}{v_t} = \frac{1}{v_0} + Kt + \frac{Kt_s}{2}(e^{-t/t_s} - 1) \quad (6)$$

where  $t_s$  is the transitional time scale. The half life is similar to Eq.4 but with a small additional term. Increasing the transitional time scale reduces the initial decay and gradually relaxes the decay rate to that of the original model, imitating the effect of the TC gradually moving over land. We also compare both the ALG and ALG-t models to the exponential model (EXP) formulated as a linear drag;

$$\frac{dv}{dt} = -\alpha v \quad (7)$$

and exponential decay,

$$v_t = v_0 e^{-\alpha t} \quad (8)$$

where  $\alpha$  is the decay constant and  $\tau = 1/\alpha$  is the decay time constant.

## 2.2 Data

The models are applied to the global International Best Track Archive for Climate Stewardship (IBTrACS) (Knapp et al., 2010, 2018) data. Starting from the IBTrACS data (for consistency we only utilise data from the USA agencies) the tracks are linearly interpolated to hourly resolution and verified to be over land (Hastings et al., 1999). We only consider storms that are at least Cat 1 ( $v_0 > 33$  m/s) at landfall over a continental landmass and are recorded for at least 24 hours over land. We only consider storms that decay and do not re-intensify. We also include 6 storms that reached peak intensity within 6 hours post landfall. With this criteria 131 TCs were available for this analysis (see Fig. S1). The 24-hour decay is then fit to each model using non-linear least squares at 6 intervals (00, 06, 12, 18 and 24 hrs at/after landfall) as in Li and Chakraborty (2020) to obtain the algebraic decay parameter  $K$ , a transition timescale  $t_s$ , and the exponential decay constant  $\alpha$ .

## 3 Results

### 3.1 Model Performance

The average decay of the maximum wind speed over land is shown for the standard algebraic decay model (ALG, Eqn. 2), modification (ALG-t, Eqn. 6), exponential decay model (EXP, Eqn. 7) and best track observations in Figure 1. While Figure 1 suggests a better mean performance for the exponential model, Table 1 shows that ALG-t has a lower mean absolute error than the exponential for most hours during the decay. The addition of a time-varying  $K$  over some timescale  $t_s$  (ALG-t) reduces the errors and bias of the original ALG model. The mean Pearson correlation ( $r^2$ ), time-averaged mean absolute error (MAE), root-mean-squared error (RMSE) and 6-24 hr mean bias or mean absolute error are also shown in Table 1. The average values of the fitted parameters for each model are;  $K = 4.22 \times 10^{-7}$  m $^{-1}$  (ALG),  $K = 5.24 \times 10^{-7}$  m $^{-1}$ ,  $t_s = 7.4$  hrs (ALG-t) and  $\alpha = 0.044$  h $^{-1}$ . Storms with  $t_s > 1$  hr have a mean  $t_s = 9.5$  hrs. This is consistent with the average translation speed over land (20 km/hr) and radius of gale force wind (200 km), which gives a transitional timescale of 10 hrs.

Overall, the performance of the physical and exponential models are similar. However, the ALG and EXP models do differ in their dependence on the initial wind speed  $v_0$  at landfall (Fig.2). We find a positive relationship between the initial landfall  $v_0$  and the value of decay constant  $\alpha$  for each storm ( $r^2=0.08$ ,  $p<0.01$ ). However, the algebraic decay parameter,  $K$ , does not depend on  $v_0$  ( $r^2=0.02$ ,  $p>0.05$ ).

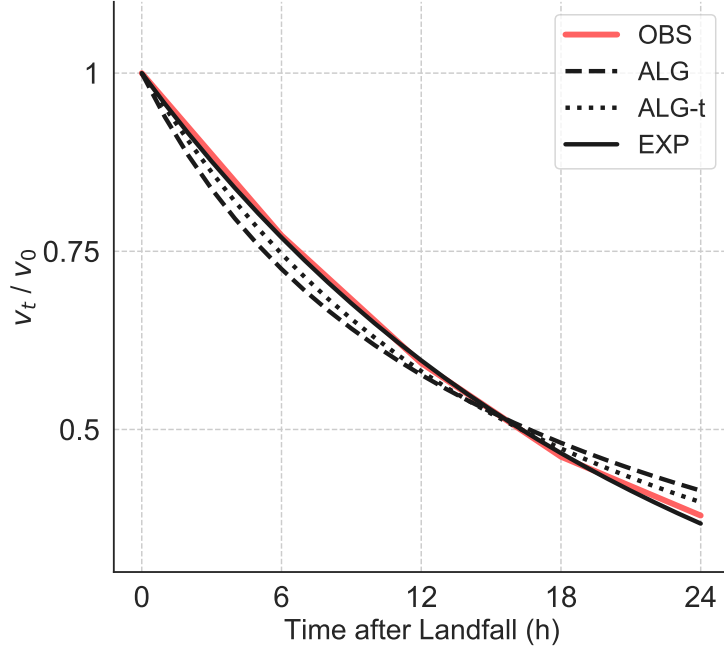


**Figure 1.** The global average maximum speed as a function of time post landfall normalised by the initial maximum speed ( $v_t/v_0$ ). Observed speed from best track data set, OBS (red solid line); the fitted algebraic model, ALG (black dashed line), the modified algebraic model, ALG-t (black dotted line) and exponential model, EXP (black solid line)

**Table 1.** Average correlation and model error of  $v_t$  in m/s. The mean Pearson correlation ( $r^2$ ), mean absolute error (MAE), root-mean-squared error (RMSE) and 6 to 24 hr mean bias (absolute error) for the standard algebraic (ALG), modified algebraic (ALG-t) and exponential (EXP) model.

Model	$r^2$	MAE	RMSE	Mean Bias (Abs. Err.)	6h	12h	18h	24h
ALG	0.96	1.5	1.9		-2.2 (2.6)	-0.7 (1.4)	0.9 (1.3)	1.6 (2.2)
ALG-t	0.97	1.1	1.4		-1.2 (1.7)	-0.5 (1.2)	0.5 (1.0)	0.9 (1.6)
EXP	0.97	1.1	1.4		-0.2 (2.0)	0.2 (1.4)	0.2 (0.9)	-0.5 (1.9)

141

### 3.2 Trends

142

143

144

145

146

147

148

149

150

Long-term trends of estimated  $K$ ,  $t_s$  and  $\alpha$  for each storm from 1980 to 2018 can also be examined.  $K$  exhibits a negative global trend of  $-0.35 \pm 0.31 \times 10^{-7} m^{-1}$  and  $-0.42 \pm 0.37 \times 10^{-7} m^{-1}$  per decade for ALG (Figure 3a) and ALG-t respectively ( $p < 0.05$ ). This shows that land falling major cyclones are decaying more slowly globally. The transitional time scale  $t_s$  of the ALG-t model fit remained unchanged at around 7 hours (not shown). The EXP model exhibits no global trend in the exponential time constant (Figure 3b). For North Atlantic (USA, Mexico, Central America) hurricane and China typhoons landfall we do not find a significant decrease in either exponential or algebraic decay constants (not shown).

151

152

153

Figure 4 shows the trends of observed maximum surface wind speed at landfall and 24 hours later. For the wind speed at landfall,  $v_0$ , a nearly significant trend of  $+1.54 \pm 1.54$  m/s ( $p=0.05$ ) is found. The wind speed further inland ( $v_6, v_{12}, v_{18}, v_{24}$ ) has also been

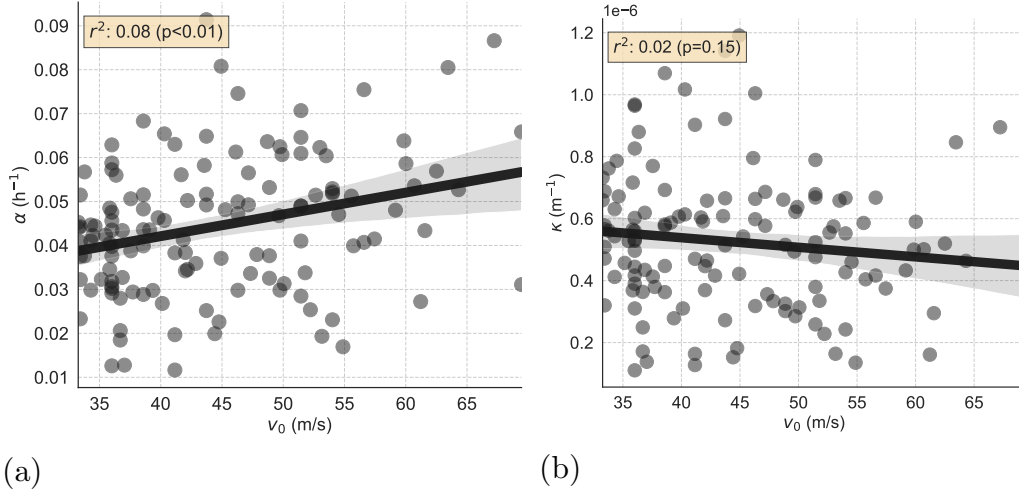


**Figure 2.** Dependence of decay parameters on the initial wind speed  $v_0$  for a) the exponential decay constant  $\alpha$  and b) the algebraic decay parameter  $K$ . A linear regression for each is highlighted as a solid line.

154 increasing. We find that the wind speed trend has the smallest error at 24 hours and has  
 155 been increasing by  $1.13 \text{ x} \pm 0.92 \text{ m/s}$  per decade ( $p=0.02$ ). This global average increase  
 156 in  $v_t$  further in land is consistent with the decrease in the decay parameter,  $K$  found ear-  
 157 lier (Fig.3a).

158 Globally averaged trends are significant only after landfall (Fig 5a). Three coun-  
 159 tries together make up the majority of land falling events in the data: the USA, China  
 160 and Australia. Wind speed increases are found at all times except in Australia. How-  
 161 ever, the significance depends on the time after landfall. For the USA the trend for the  
 162 wind speed becomes significant at the end of decay at 24 h (Fig 5b). For China signif-  
 163 icance is only found at landfall (Fig 5c).

#### 164 4 Discussion

165 We analysed the global decay of tropical cyclones post landfall. The statistical per-  
 166 formance of the physically based algebraic model of TC decay and a small correction for  
 167 the ocean to land transition perform statistically very similar to the widely used empir-  
 168 ical exponential model. This is the first time decay models have been compared for a global  
 169 data set and highlights that the algebraic model could enable a physical interpretation  
 170 of post landfall TC wind speed evolution.

171 Kaplan and DeMaria (1995) showed that the exponential exponent depends on the  
 172 initial value. This has been confirmed by subsequent studies in the USA and elsewhere  
 173 (Kaplan & DeMaria, 2001; Bhowmik et al., 2005; Wong et al., 2008). We also find that  
 174 the correlation of an exponential decay coefficient with  $v_0$  globally is small but signif-  
 175 icant. Similar correlation coefficients were found by Wong et al. (2008) for the South China.  
 176 However, this behaviour is mathematically inconsistent with a proposed simple exponen-  
 177 tial decay, which requires a time constant independent of the initial value. Empirical ad-  
 178 justments that are frequently applied to correct for this are thus a recognition of this model's  
 179 inadequacy. This is perhaps not surprising as theoretically an exponential model would  
 180 be appropriate for laminar boundary layer, but for TC eye wall conditions a turbulent

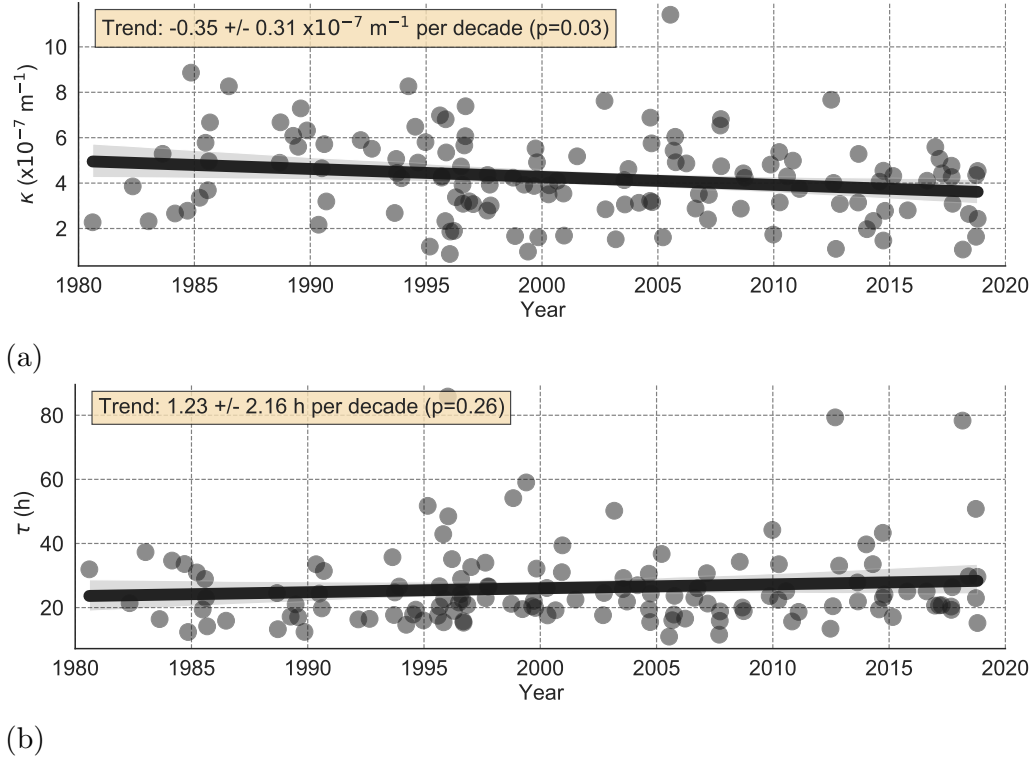


**Figure 3.** Time series of the decay parameters for each landfall (1980-2018) with a linear regression line, trend and p-value in the figure: a) the ALG decay parameter  $K$  ( $m^{-1}$ ); b) the exponential time constant  $\tau$  (h) ( $=1/\alpha$ ).

181 layer is much more plausible. Turbulent surface drag underpins the algebraic decay model.  
 182 In our framework the algebraic decay parameter  $K$  does not depend on the  $v_0$ .

183 The decay parameter  $K$  is essentially controlled by the ratio of two physical quantities:  
 184 the surface drag co-efficient and the effective vortex depth which is being spun down.  
 185 The land surface drag coefficient is very uncertain. This is partly due to the complex-  
 186 ity of land surface, but there is also evidence of a decreasing drag coefficient for increas-  
 187 ing wind speed and increased instability (Srivastava & Sharan, 2015). They suggest that  
 188 the drag coefficient at 10 m/s for tropical convective conditions could be about  $3.0 \times 10^{-3}$ .  
 189 Is the algebraic model consistent with a reasonable estimate of an effective vortex depth  
 190 ? For a global mean value of  $K$  of about  $5 \times 10^{-7} m^{-1}$ ,  $\chi = 0.8$  (Powell, 1980), and  
 191 a  $C_D = 3 \times 10^{-3}$  then an effective vortex depth,  $H$ , of about 5 km would be inferred.  
 192 This crudely estimated height is at least plausible as the depth over which the vortex  
 193 is spin down given all the uncertainties and simplifications.  $H$  may approximate to half  
 194 the height of the tropopause or the height of half-maximum  $v_0$  and could remain constant  
 195 during the decay. The advantage of the algebraic model over the empirical expo-  
 196 nential decay is that because it has a physical framework the relevant physical variables  
 197 can be interpreted. A full physics model will capture more details of the boundary layer  
 198 and its parameterisation (Zhang & Pu, 2017; Zhang et al., 2021).

199 We find a decrease in observed global average post landfall decay. For example, a  
 200 tropical cyclone with  $v_0 = 33$  m/s (Cat 1) in the 1980s would have a half life (time to  
 201 decay to 17 m/s i.e. a gale force strength wind) of around 16 hours. By now this Cat  
 202 1 storm would have a much larger half life of 23 hours. This increase could amount to

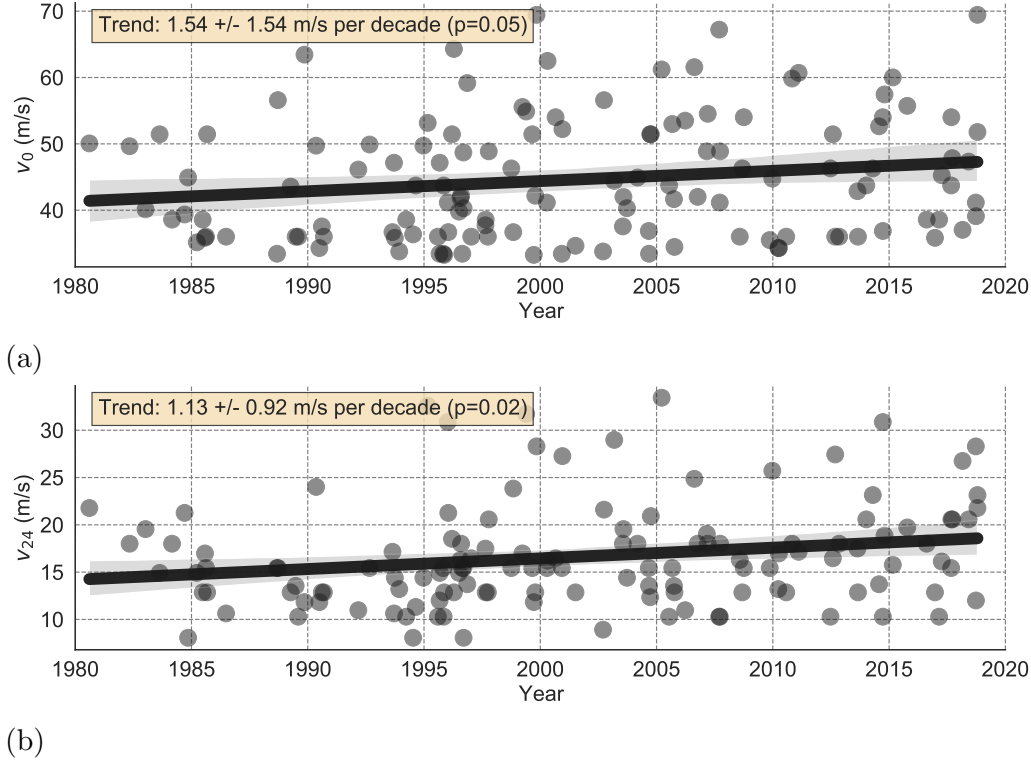


**Figure 4.** Time series of  $v_t$  (m/s) of each landfall event globally (1980-2018) with a linear regression line, trend and p-value for a)  $v_0$ ; and b)  $v_{24}$ ; .

203 much more damage in land with an extra 7 hours of gale force winds. It is interesting  
 204 to note that under the algebraic framework the half-life decreases with more intense ini-  
 205 tial landfall intensity (Eqn. 4). There is an element of self-regulation: in-land wind speed  
 206 changes are mitigated by the shorter half-life of any potential increase in initial landfall  
 207 intensity (Wang et al., 2020).

208 This is the first time a global average trend in landfall decay is presented. For North  
 209 Atlantic (USA, Mexico, Central America) hurricane landfall we do not find a significant  
 210 decrease in either exponential or algebraic decay constants. This appears to be in dis-  
 211 agreement with the recent study of Li and Chakraborty (2020). However, if we adopt  
 212 their criteria and allow storms that re-intensify after an initial decay we do then also find  
 213 a trend in the exponential time scale of  $+5.0 \pm 4.7$  hr per decade ( $p=0.04$ ) and this agrees  
 214 with their 3 hr/decade trend. Re-intensification appears to explain a large part of their  
 215 trends. For landfall in China we find no change in algebraic decay parameters or expo-  
 216 nential time constant. This is consistent with the lack of trend of the weakening rate over  
 217 the same time period as reported by Liu et al. (2020).

218 The wind speed at different times post-landfall is increasing by about 1 m/s per  
 219 decade on average globally. An analysis of three countries which account for most of the  
 220 global landfall shows differences between them. There is no significant change in Aus-  
 221 tralia. Although there is an increased wind speed at all times for the USA and China,  
 222 the significance depends on the time post landfall. The small sample size makes it dif-  
 223 ficult to detect trends at country level.



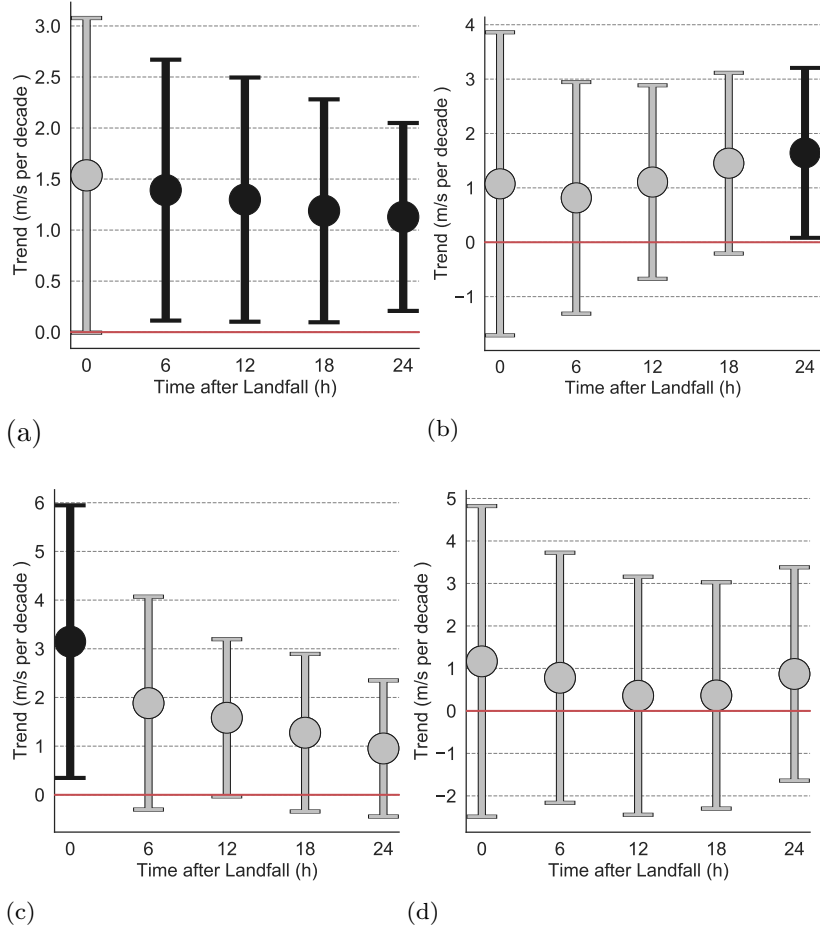


**Figure 5.** Global and country  $v_t$  trends (m/s per decade) with 95% confidence intervals for different times (0-24hr). The trends highlighted in black indicate significance at  $p=0.05$ . The zero trend marker is highlighted as a solid red line. a) Global (131 events). b) USA (29 events). c) China (32 events). d) Australia (27 events).

224 Is the  $v_{24}$  increase mostly driven by the  $v_0$  at landfall or the decay parameter? If  
 225 we assume no change in  $v_0$  and the observed trend  $K$  of  $-0.35 \pm -0.31 \times 10^{-7}$  per decade  
 226 then, according to Eq .2 the  $v_{24}$  trend would be  $+0.92 \pm 0.84$  m/s per decade and thus  
 227 close the observations ( $+1.13 \pm 0.92$  m/s per decade). However, for no change in  $K$  and  
 228 assuming a  $v_0$  trend of  $+1.54 \pm 1.54$  m/s per decade this would produce a trend of  $v_{24}$   
 229 of  $+0.56 \pm 0.56$  m/s per decade, still within the error of the observed  $v_{24}$  trend. We can  
 230 therefore not exclude the possibility that the inland trend is caused by a change of  $v_0$ ,  
 231 but our best estimate (smallest error in trend) is that it is the slowing decay that is re-  
 232 sponsible.

233 Li and Chakraborty (2020) attribute enhanced atmospheric moisture from ocean  
 234 surface warming as the cause of the slowing decay of hurricane land decay. In our frame-  
 235 work enhanced moisture could slow the decay by increasing  $H$  through enhanced latent  
 236 heating in the eye wall. Komaromi and Doyle (2017) report a strong positive relation-  
 237 ship between outflow potential temperature (a measure of height) and the mean equiv-  
 238 alent potential temperature of the boundary layer inflow. Recent moisture enhancement

could thus have lead to either stronger  $v_0$  or larger  $H$ . However, the physical framework identifies  $v_0$  and  $H$  as two different variables that are not necessarily always linked.

## 5 Conclusion

We have shown that a simple, physically based, decay model can be useful for modelling the decay of tropical cyclone post landfall. We propose a small modification that accounts for the land roughness increase during the cyclone movement from partially to fully over land. The empirical exponential decay model, widely utilised for tropical cyclone land decay studies, does not perform much better than this physical interpretation, but does have some theoretical and practical limitations. Observations show a recent increase in wind speed post landfall and a longer time of gale force winds over land. We can not exclude the possibility that this is due to increases in intensity at landfall, but our best estimate is that the in-land increased wind speed is due to a slowing of the decay.

## Acknowledgments

Datasets for this research are available through Knapp et al. (2018). The authors acknowledge funding from the U.K.–China Research and Innovation Partnership Fund through the Met Office Climate Science for Service Partnership (CSSP) China as part of the Newton Fund.

## References

- Bhatia, K. T., Vecchi, G. A., Knutson, T. R., Murakami, H., Kossin, J., Dixon, K. W., & Whitlock, C. E. (2019). Recent increases in tropical cyclone intensification rates. *Nature Communications*, *10*(1), 635. doi: 10.1038/s41467-019-08471-z
- Bhowmik, S. K. R., Kotal, S. D., & Kalsi, S. R. (2005). An empirical model for predicting the decay of tropical cyclone wind speed after landfall over the indian region. *Journal of Applied Meteorology*, *44*(1), 179 - 185. doi: 10.1175/JAM-2190.1
- Bloemendaal, N., Haigh, I. D., de Moel, H., Muis, S., Haarsma, R. J., & Aerts, J. C. J. H. (2020). Generation of a global synthetic tropical cyclone hazard dataset using storm. *Scientific Data*, *7*(1), 40. doi: 10.1038/s41597-020-0381-2
- Chen, J., & Chavas, D. R. (2020). The transient responses of an axisymmetric tropical cyclone to instantaneous surface roughening and drying. *Journal of the Atmospheric Sciences*, *77*(8), 2807 - 2834. doi: 10.1175/JAS-D-19-0320.1
- Coch, N. K. (2020). Inland Damage from Hurricanes. *Journal of Coastal Research*, *36*(5), 1093 - 1105. doi: 10.2112/JCOASTRES-D-20A-00002.1
- DeMaria, M., Knaff, J. A., & Kaplan, J. (2006). On the decay of tropical cyclone winds crossing narrow landmasses. *Journal of Applied Meteorology and Climatology*, *45*(3), 491 - 499. doi: 10.1175/JAM2351.1
- DeMaria, M., Mainelli, M., Shay, L. K., Knaff, J. A., & Kaplan, J. (2005). Further improvements to the statistical hurricane intensity prediction scheme (ships). *Weather and Forecasting*, *20*(4), 531 - 543. doi: 10.1175/WAF862.1
- Eliassen, A. (1971). On the ekman layer in a circular vortex. *Journal of the Meteorological Society of Japan. Ser. II*, *49A*, 784-789. doi: 10.2151/jmsj1965.49A.0\_784
- Eliassen, A., & Lystad, M. (1977). The Ekman layer of a circular vortex - A numerical and theoretical study. *Geophysica Norvegica*, *31*(7), 1-16.
- Greenspan, H. P., & Howard, L. N. (1963). On a time-dependent motion of a rotating fluid. *Journal of Fluid Mechanics*, *17*(3), 385-404. doi:

- 288 10.1017/S0022112063001415
- 289 Hastings, D. A., Dunbar, P. K., Elphinstone, G. M., Bootz, M., Murakami, H.,  
 290 Maruyama, H., . . . MacDonald, J. S. (1999). *The Global Land One-*  
 291 *kilometer Base Elevation (GLOBE) Digital Elevation Model Version 1.*  
 292 NOAA National Geophysical Data Center Information. Retrieved from  
 293 <http://www.ngdc.noaa.gov/mgg/topo/globe.html>
- 294 Kaplan, J., & DeMaria, M. (1995). A simple empirical model for predicting the  
 295 decay of tropical cyclone winds after landfall. *Journal of Applied Meteorology*  
 296 *and Climatology*, 34(11), 2499 - 2512. doi: 10.1175/1520-0450(1995)034<2499:  
 297 ASEMFP>2.0.CO;2
- 298 Kaplan, J., & DeMaria, M. (2001). On the decay of tropical cyclone winds after  
 299 landfall in the new england area. *Journal of Applied Meteorology*, 40(2), 280 -  
 300 286. doi: 10.1175/1520-0450(2001)040<0280:OTDOTC>2.0.CO;2
- 301 Knaff, J. A., & Sampson, C. (2009). Southern hemisphere tropical cyclone intensity  
 302 forecast methods used at the joint typhoon warning center, part ii: statistical -  
 303 dynamical forecasts. *Australian Meteorological and Oceanographic Journal*, 58,  
 304 9-18.
- 305 Knaff, J. A., Sampson, C. R., & DeMaria, M. (2005). An operational statistical ty-  
 306 phoon intensity prediction scheme for the western north pacific. *Weather and*  
 307 *Forecasting*, 20(4), 688 - 699. doi: 10.1175/WAF863.1
- 308 Knapp, K. R., Diamond, H. J., Kossin, J. P., Kruk, M. C., & Schreck, C. J. I.  
 309 (2018). *International Best Track Archive for Climate Stewardship (IBTrACS)*  
 310 *Project, Version 4.* NOAA National Centers for Environmental Information.  
 311 (Accessed June 2020) doi: <https://doi.org/10.25921/82ty-9e16>
- 312 Knapp, K. R., Kruk, M. C., Levinson, D. H., Diamond, H. J., & Neumann, C. J.  
 313 (2010). The international best track archive for climate stewardship (ibtracs):  
 314 Unifying tropical cyclone data. *Bulletin of the American Meteorological Soci-*  
 315 *ety*, 91(3), 363 - 376. doi: 10.1175/2009BAMS2755.1
- 316 Komaromi, W. A., & Doyle, J. D. (2017, APR). Tropical cyclone outflow and warm  
 317 core structure as revealed by hs3 dropsonde data. *Monthly Weather Review*,  
 318 145(4), 1339-1359. doi: 10.1175/MWR-D-16-0172.1
- 319 Li, L., & Chakraborty, P. (2020, Nov 01). Slower decay of landfalling hurricanes in a  
 320 warming world. *Nature*, 587(7833), 230-234. doi: 10.1038/s41586-020-2867-7
- 321 Liu, L., Wang, Y., Zhan, R., Xu, J., & Duan, Y. (2020). Increasing destructive po-  
 322 tential of landfalling tropical cyclones over china. *Journal of Climate*, 33(9),  
 323 3731 - 3743. doi: 10.1175/JCLI-D-19-0451.1
- 324 Montgomery, M. T., Snell, H. D., & Yang, Z. (2001). Axisymmetric spindown dy-  
 325 namics of hurricane-like vortices. *Journal of the Atmospheric Sciences*, 58(5),  
 326 421 - 435. doi: 10.1175/1520-0469(2001)058<0421:ASDOHL>2.0.CO;2
- 327 Powell, M. D. (1980). Evaluations of diagnostic marine boundary-layer models ap-  
 328 plied to hurricanes. *Monthly Weather Review*, 108(6), 757 - 766. doi: 10.1175/  
 329 1520-0493(1980)108<0757:EODMBL>2.0.CO;2
- 330 Smith, R. K., & Montgomery, M. T. (2008). Balanced boundary layers used in hurri-  
 331 cane models. *Quarterly Journal of the Royal Meteorological Society*, 134(635),  
 332 1385-1395. doi: <https://doi.org/10.1002/qj.296>
- 333 Srivastava, P., & Sharan, M. (2015). Characteristics of the drag coefficient over a  
 334 tropical environment in convective conditions. *Journal of the Atmospheric Sci-*  
 335 *ences*, 72(12), 4903 - 4913. doi: 10.1175/JAS-D-14-0383.1
- 336 Vickery, P. J. (2005). Simple empirical models for estimating the increase in the  
 337 central pressure of tropical cyclones after landfall along the coastline of the  
 338 united states. *Journal of Applied Meteorology*, 44(12), 1807 - 1826. doi:  
 339 10.1175/JAM2310.1
- 340 Vogl, S., & Smith, R. K. (2009). Limitations of a linear model for the hurricane  
 341 boundary layer. *Quarterly Journal of the Royal Meteorological Society*,  
 342 135(641), 839-850. doi: <https://doi.org/10.1002/qj.390>

- 343 Wang, S., Rashid, T., Throp, H., & Toumi, R. (2020). A shortening of the life  
344 cycle of major tropical cyclones. *Geophysical Research Letters*, *47*(14),  
345 e2020GL088589. doi: <https://doi.org/10.1029/2020GL088589>
- 346 Wang, S., & Toumi, R. (2021). Recent migration of tropical cyclones toward coasts.  
347 *Science*, *371*(6528), 514–517. doi: [10.1126/science.abb9038](https://doi.org/10.1126/science.abb9038)
- 348 Wong, M. L. M., Chan, J. C. L., & Zhou, W. (2008). A simple empirical model  
349 for estimating the intensity change of tropical cyclones after landfall along the  
350 south china coast. *Journal of Applied Meteorology and Climatology*, *47*(1), 326  
351 - 338. doi: [10.1175/2007JAMC1633.1](https://doi.org/10.1175/2007JAMC1633.1)
- 352 Zhang, F., & Pu, Z. (2017). Effects of vertical eddy diffusivity parameterization on  
353 the evolution of landfalling hurricanes. *Journal of the Atmospheric Sciences*,  
354 *74*(6), 1879-1905. doi: [10.1175/JAS-D-16-0214.1](https://doi.org/10.1175/JAS-D-16-0214.1)
- 355 Zhang, F., Pu, Z., & Wang, C. (2021). Land-surface diurnal effects on the asym-  
356 metric structures of a postlandfall tropical storm. *Journal of Geophysical*  
357 *Research: Atmospheres*, *126*(1), 2020JD033842. doi: [https://doi.org/10.1029/](https://doi.org/10.1029/2020JD033842)  
358 [2020JD033842](https://doi.org/10.1029/2020JD033842)